

Table 6.9 Global statistics of all 4 options for comparison

		Alignment Alternative I-5		Alignment Alternative AV	
		Max. grade 3.5%	Max. grade 2.5%	Max. grade 3.5%	Max. grade 2.5%
Construction time analysis	Unit	Value	Value	Value	Value
Number of simulations	[-]	1000	1000	1000	1000
Mean value	[working days]	2218	2124	1125	1430
Median value	[working days]	2111	2027	1089	1321
St. Deviation	[working days]	471	431	217	370
Minimum value	[working days]	1492	1470	962	1060
Value at 95%	[working days]	3100	2900	1250	2050
Difference between 95% value and mean value	[working days]	882	776	125	620
Difference between 95% value and min value	[working days]	1608	1430	288	990
Coefficient of Variation	[%]	21.2	20.3	19.3	25.9
Construction cost analysis	Unit	Value	Value	Value	Value
Number of simulations	[-]	1000	1000	1000	1000
Mean value	[US\$ x 1000]	1670080	1779101	1127511	1614790
Median value	[US\$ x 1000]	1643417	1758361	1125936	1610143
St. Deviation	[US\$ x 1000]	133507	110232	21023	34021
Minimum value	[US\$ x 1000]	1420421	1576264	1073210	1537212
Value at 95%	[US\$ x 1000]	1925000	1975000	1150000	1675000
Difference between 95% value and mean value	[US\$ x 1000]	254920	195899	22489	60210
Difference between 95% value and min value	[US\$ x 1000]	504579	398736	76790	137788
Coefficient of Variation	[%]	8.0	6.2	1.9	2.1

6.4 Discussion of the Results

The results obtained from the DAT simulations must be correctly interpreted in the light of the underlining assumptions.

Considering the variation in the total construction costs (see Figure 6.13 and Table 6.9), it can be observed that, for both Alignment alternatives there is a clear positive relationship between the increase in the average cost and the total length of tunneling (when changing from the 3.5%-max-grade to the 2.5%-maximum grade), as one would normally expect.

Considering the uncertainty about costs which can be measured by the Coefficients of Variation, see Table 6.9), both maximum grade options of the I-5 alignment show higher dispersion than those of the corresponding AV alignment which can be attributed to the more adverse, geologic conditions found along the I-5 alignment.

Additionally, the augmented tunneling length for the AV alignment implies an increase in the spread of results (COV from 1.9% to 2.1%), which is consistent with the increased uncertainties associated with more tunnel stretches running through geologically difficult zones. [Considering the actual tunnel configurations which do not differ from the 2.5% to the 3.5% maximum grade option, the opposite trend of COV, from 8.0% to 6.2%, is evident for the I-5 alignment.]

Similar considerations can be made about the total construction times, especially for the I-5 alignment. The reduced average total construction time for the 2.5% maximum grade configuration, which has approximately 1.5 miles of more tunneling than the 3.5% configuration, derives from the different construction schemes adopted, where one more TBM had to be introduced to optimize the whole construction scheme.

In addition to the above general comments, the following specific observations can be made:

- 1) The shape of the clouds for the AV alignment (both 3.5% and 2.5% grade options), as shown in the comparative scatter plot of Figure 6.13, is quite different from those of the I-5 alignment (both grade options).

In the case of the AV Alignment, the cloud tends to close down towards the high ends (of time and cost) with increasingly fewer number of points, while that of the I-5 Alignment is not only wider but also open, with a lower concentration of results in the desired lower range of total construction cost and duration.

Without entering into the statistical data and the absolute values, the discrepancy above means that the uncertainty of the result in the I-5 alignment is much higher than in the AV alignment.

- 2) For all four options studied, the dispersion of results is always wider in the time direction than in the cost direction. This is because a linear correspondence between an increase of time and an increase of costs is not foreseen. For tunnel excavation by TBM, supported by pre-cast concrete lining, there is a wide variation in the advance rate due to variations in ground conditions. However, there is no significant variation in the construction cost per linear meter of tunnel. For the HSR Project, the combination of TBM excavation with pre-cast concrete lining is the construction method adopted for almost all tunnels involved in each option.

- 3) The scattering aspect revealed in Item 1) above is shown clearly by the histograms, especially in the area of costs. Both grade options of the AV Alignment have an extremely “slim” distribution (see Figures 6.9 and 6.12) of cost, with quite small differences between the 95% value and the minimum value (being 76 millions of USD for the 3.5% maximum grade option and 137 millions of USD for the 2.5% maximum grade option, respectively, see Table 6.6 and Table 6.8). The same results are much more uncertain for the I-5 Alignment, with very large differences between the 95% value and the minimum value (being 500 millions of USD and 400 millions of USD for the 3.5%, see Table 6.2, and the 2.5% maximum grade option, see Table 6.4, respectively.)
- 4) In terms of the mean construction cost, the 3.5% maximum grade option of the AV alignment is about 40% cheaper than that of the corresponding I-5 alignment, while this advantage is reduced for the 2.5% maximum grade option, being about 15% cheaper, due to the increased total length of tunnelling works involved. Furthermore, it should be noted that the increased tunnel length for the AV alignment at the 2.5% maximum grade means savings in costs for construction of the external works and for the mitigation of the environmental impact in the stretches replaced by tunnels.
- 5) The time histograms of both maximum grade options of the I-5 alignment have similar distributions (see Figure 6.2 and Figure 6.5), due to the fact that the differences in the construction schemes do not affect the final construction time. The main difference consists in the existence of a second set of seismic chambers to cross the San Andrea Fault Zone. This feature introduces additional, costs, but not time because the construction of the second couple of seismic chambers was foreseen to be done mainly during the long period of procurement and assembly of the TBMs. The TBMS will start their tunnel excavation from the chambers and, thus will not affect the final construction time.
- 6) The 2.5% maximum grade option of the AV alignment has a consistently lower range of variation in the total construction time (with a difference of 990 working days between the 95% value and the minimum value, see Table 6.7), and the 3.5% maximum grade option has an even lower range (being only 288 working days, see Table 6.5). However, the corresponding differences for the I-5 alignment are 1608 and 1430 working days respectively for the 3.5% (see Table 6.1) and the 2.5% maximum grade option (see Table 6.3). These differences between the AV and the I-5 alignment derive mainly from the differences in the geological conditions involved: the relatively shorter and shallower tunnels on the AV alignment are associated with less geological difficulties and thus a lower degree of uncertainty, compared with the long and deep tunnels on the I-5 Alignment.
- 7) For the 3.5% maximum grade option, the mean construction time required for the I-5 alignment is almost twice as much as that required for the AV alignment (2218 working days against 1125 working days, see Table 6.9). The same trend is basically true also for the 2.5% maximum grade option, with a slight increase in the mean construction time for the AV alignment, due to increased total length of tunneling (see also Table 3.1).
- 8) It should be pointed out that our DAT analysis does not simulate the financial consequences associated with increased construction duration which could change significantly the forecast of the total investment cost. This financial impact of

construction duration will definitely further magnify the current differences in the construction costs between the I-5 options and the AV options.

Finally, with reference to all the histograms fitted with a cumulative normal distribution curve, the risk of exceeding certain cost or time limits can be easily evaluated if such limits or targets are known.

The conclusions derived from the DAT-simulation results are presented in Section 7.

7. CONCLUSIONS AND RECOMMENDATIONS

Given the large amount of tunneling works involved (see Table 3.1), the Bakersfield to Los Angeles Corridor itself, be it the I-5 alignment or the Antelope Valley alignment, is a mega project.

The potential, typical risks that may be encountered in a mega tunneling project are:

- 1) Risk of encountering adverse conditions due to the inherent uncertainties of ground and groundwater conditions – leading to significant cost overruns and project delay;
- 2) The potential for accidents during tunneling work and, later on, during operation;
- 3) Risk to the health and safety of workers and third party individuals, including personal injury and, in extreme cases, loss of life;
- 4) Construction risks, such as choice of a wrong type of TBM, ground-squeezing behavior, face collapses; and production of materials causing hazardous environmental conditions;
- 5) Financial risks to the owner, such as delay in completion of the contract or cost overruns;
- 6) Contractual risks, such as additional work not covered, time delays, disputes, claims and litigation.

The underground construction industry seems particularly prone to disputes. This is most likely because of the risks and uncertainties associated with subsurface conditions and the costly plant and equipment required (for example, the TBM and its associated back up gear).

Traditionally, the potential risks listed above have been managed indirectly through the engineering decisions taken during project development. This approach is often found to be inadequate during construction. Many recent case histories have demonstrated that risk management can be significantly improved by using systematic risk management techniques throughout the tunneling project development. The use of these techniques can ensure that most potential problems are identified and addressed in a timely fashion so that appropriate and cost effective risk reducing measures can be implemented. The use of risk management in the early stages of a tunnel project is essential, particularly at the beginning of the planning process where major decisions, such as choice of alignment and selection of construction methods, can be influenced.

The study presented in this report was commissioned for two main reasons, (1.) Specific uncertainties in the tunneling process were not adequately integrated in earlier studies commissioned by the Authority, and (2.) to identify the optimum alignment with respect to minimizing capital investment and risk of construction cost overruns and costly delays.

As pointed out in Section 1.2.2, the earlier studies of the Authority have focused on minimizing tunnel requirements and cost (Corridor Evaluation study and QUANTM study) and minimizing potential environmental impacts (the Screening Evaluation) by

avoiding sensitive zones in identifying the potentially suitable routes. However, there is a limit to these reductions due to the constraints imposed by the specific topography and tectonic setting of the region as well as the high speed train technology. Furthermore, for the limited number of potentially suitable routes identified by the previous screening studies, and subsequently confirmed by the QUANTM analysis, the various categories of risks, especially the geological and construction risks, were not considered. In the opinion of Transmetrics/Geodata, these other risks are as important as those already considered by the Authority. They are also critical in the final choice of the optimum alignment/route for the mega tunneling project.

Consequently, the study commissioned by the City of Palmdale and undertaken by Transmetrics/Geodata represents a complementary, step forward in the development process of the Project.

It is understood from the beginning of this report that, to perform an alignment specific risk analysis, focusing on the geological and constructional aspects, requires specific information about the ground conditions of each potentially suitable alignment. However, most of the required information is not directly available because no preliminary site-specific investigations have been made.

To overcome this problem, we adopted the common practice of utilizing our tunneling experience and judgment as well as USGS data and reports in lieu of precise, in situ explorations and measurements. In addition, full use was made of the information contained in the Preliminary Engineering Feasibility Study of PBQD. We acquired relevant reports and maps from the USGS to study the geomorphological, geological, hydrogeological, and geotechnical conditions of the two alternative alignment corridors, establishing foreseeable ground models. We also made a preliminary design of both alignments, defining the corresponding construction schemes based on our European experience for similar projects.

To facilitate the comparison of the geological and construction risks involved in the two alternative alignments and also to further overcome the problem of limited data, we adopted a probabilistic model that incorporates the impact of different geological factors on the risks and productivity. The specific model adopted was developed at the Massachusetts Institute of Technology and is called Decision Aids in Tunneling (DAT). The model allows for the comparison, in terms of construction time and cost, of various, feasible, design and construction solutions for a tunneling project, and for quantification of risks related to each solution.

The various analyses presented in this report have demonstrated the following:

- Although the amount of tunneling work involved in the I-5 and the AV alignment are almost the same, be it the 2.5% grade or the 3.5% grade option, the ground conditions along the AV are relatively more favorable and hence involve less construction risks, financial risks, and contractual risks.
- For the 3.5% max grade option, the mean construction time required for the I-5 alignment is almost twice as much as that required for the AV alignment (2218 working days against 1125 working days, see Table 6.9). The same trend is basically true for the 2.5% max grade option, with a slight increase in the mean construction time for the AV alignment due to increased total length of tunneling (see also Table 3.1).

- In terms of the mean construction cost, for the 3.5% max grade option, the Antelope Valley alignment is about 40% cheaper than the I-5 alignment, while this advantage is reduced for the 2.5% max grade option. The 2.5% grade option is 15% cheaper, again due to increased total length of the tunnel. Furthermore, the increased tunnel length for the AV alignment at 2.5% max grade will reduce the costs for the corresponding external works and environmental impact.
- It should be pointed out that the DAT analyses presented in this report do not simulate the financial consequences associated with increased construction duration. If the financial impact due to longer construction duration is taken into consideration, the final results will not only change significantly the forecast of the total investment required for each alignment option, but will also magnify the construction cost differences between the I-5 and the Antelope Valley alignment.

Generally speaking, the findings of this study have confirmed the concerns of the City of Palmdale over the relative risks involved in the two alternative alignments. These findings should also permit the Authority to make more informed decisions regarding the final choice of the best alignment, including the process to be followed before making the final choice.

On the basis of the analysis conducted, we offer the following three specific recommendations:

In general, the construction experience gained by Geodata from similar, International, mega projects is directly useful as information to assist consideration of new alternatives – management, contracting and new technologies – for the current mega project.

1) Reducing uncertainties

Reducing uncertainties through site investigations, especially the preliminary investigation, for mechanized tunneling, is a key investment strategy for project owners because it will directly reduce risks with short, medium and long term benefits.

To facilitate the final choice of the optimum alignment, site investigations should be designed to reduce the geological uncertainties, thus either confirming or negating the geological and construction risks identified in the analyses presented in this report. For this purpose, a proper balance of effort should be maintained between investigating the I-5 alignment and exploring the Antelope Valley alignment.

Once the optimum alignment is selected, it is strongly recommended that critical sections (if not all sections) of the service tunnels should be constructed first, since they can be used as pilot tunnels to investigate the ground conditions and to experiment with the construction techniques to be employed for the construction of the main tunnels later.

2) Development of Innovation – New Technologies

The greatest payoff can be realized by the use of innovation in complex underground projects, especially long and deep tunnels, with difficult or unexplored geology, as in the California High Speed Rail project. In addition to the risks listed previously, there are still potential technological risks. For example, the technical feasibility of realizing the huge, seismic chambers in very wide fault zones, and the technical capacity of the tunneling market to supply the great number of large-diameter TBM's required for realizing this mega tunneling project will be a challenging task.

Innovation means that the new concepts are competently developed, consistent with the limits of current knowledge and experience, and carefully matched to the specific conditions of the project. For this purpose, it is suggested that the Authority work closely with engineers, contractors and manufacturers, as early as possible, to develop innovative solutions to the high risk aspects of the project, bearing in mind that innovation takes time.

3) Contracting Practices

It is now almost universally accepted that “the ground belongs to the Owner” – including the sometimes unknown difficult geologic conditions which will be encountered. Wise Owners recognize this and seek ways to equitably mitigate the risks, sharing and allocating risk to the best entity that can foresee or control that particular risk. Passing risk along without a strategic and equitable approach will often lead to disputes which will eventually have a great impact on the project and the Owner.

It is now accepted by many Owners that the contracting practice of accepting a fixed-cost low bidder from a group of “qualified” contractors, should not be adopted when the jobs are large, the geology uncertain, and potential for extremely high cost overruns escalate. It has been the experience of some Owners that the low-bid contracting system can result in delays, cost overruns, problems with project completion and a long process of claims and litigation. Negotiated contracts with fair allocation of risks among the parties involved could be more cost effective and equitable.

Appendix 1 List of reference geological documents

Type	Title	Year of publ.	Other	
Map	Geologic map of the Warm Springs Mountain Quadrangle	1997		scale 1:24,000
Map	Geologic map of the Whitaker Peak Quadrangle	1997		scale 1:24,000
Map	Geologic map of California. Los Angeles sheet	1969		scale 1:250,000
Map	Geologic map of California. Bakersfield sheet	1965		scale 1:250,000
Map	Geologic map of California	1977		scale 1:750,000
Map	Geologic map and cross sections of the southeastern margin of the San Joaquin Valley, California	1984		scale 1:125,000 (contains Bakersfield area)
Map+Paper	Geologic map of the Tehachapi Quadrangle, Kern County, California	1970		scale 1:65,000 (with accompanying explanatory paper)
Map	Geologic map of the San Andreas Fault Zone, Leona Valley, California	1976 (repr. 1984)		scale 1:10,000
Paper+Maps	Geology of the Willow Springs and Rosamond Quadrangles, California	1963		scale 1:62,500
Map+Paper	Geologic map of the Cummings Mountain Quadrangle, Kern County, California	1970		scale 1:65,000 (with accompanying explanatory paper)
Map	Geologic map of the Pearland Quadrangle, California	1953		scale 1:24,000 relevant descriptive notes on the map
Map	Geologic map of the Black Mountain Quadrangle, California	2002		scale 1:24,000
Map	Geologic map of the Liebre Mountain Quadrangle, California	2002		scale 1:24,000
Map	Geologic map of the Pacifico Mountain and Palmdale (south half) Quadrangle, California	2001		scale 1:24,000
Map	Geologic map of the Sleepy Valley and Ritter Ridge Quadrangles, California	1997		scale 1:24,000
Paper+Map	Postcrystalline Deformation of the Pelona Schist Bordering Leona Valley, Southern California	1978	Geological Survey Professional Paper 1039 with annexed geologic map at 1:10,000	
Paper+Map	Basement-Rock Correlations Across the White Wolf-Breckenridge-Southern Kern Canyon Fault Zone, Southern Sierra Nevada, California	1986	U.S. Geological Survey Bull. 1651, with annexed geologic map at 1:25,000	
Paper+Map	Stratigraphy and Sedimentology of the Eocene Tejon Formation, Western Tehachapi and San Emigdio Mountains, California	1987	U.S. Geological Survey Bull. 1268, with annexed geologic non colour map at 1:62,500	
Paper+Map	The Metamorphic and Plutonic Rocks of the Southermost Sierra Nevada, California, and their Tectonic Framework	1989	U.S. Geological Survey Professional Paper 1381, with annexed geologic map at 1:125,000	
Map	Geologic map of the Grapevine Quadrangle, California	1973	U.S. Geological Survey open file map, preliminary non colour. Scale 1:24,000	
Map	Geologic map of the Pastoria Creek Quadrangle, California	1973	U.S. Geological Survey open file map, preliminary non colour. Scale 1:24,000	
Map	Geologic map of the Eagle Rest Peak Quadrangle, California	1973	U.S. Geological Survey open file map, preliminary non colour. Scale 1:24,000	
Map	Geologic map of the Santiago Creek Quadrangle, California	1973	U.S. Geological Survey open file map, preliminary non colour. Scale 1:24,000	
Map	Geologic map of the Pleito Hills Quadrangle, California	1973	U.S. Geological Survey open file map, preliminary non colour. Scale 1:24,000	
Maps (4)+Table	Geologic maps of the Knob Hill, Pine Mountain, Oil Center and Bena Quadrangles, California	1986	U.S. Geological Survey open-file report 86-188, preliminary non colour. Scale 1:24,000	
Map+Notes	Preliminary Geologic map of the Val Verde 7.5' Quadrangle, Southern California	1995	U.S. Geological Survey open-file report 95-504, preliminary non colour. Scale 1:24,000	
Map+Notes	Preliminary Geologic map of the Oat Mountain 7.5' Quadrangle, Southern California	1995	U.S. Geological Survey open-file report 95-89, preliminary colour. Scale 1:24,000	
Map+Notes	Preliminary Geologic map of the Mint Canyon 7.5' Quadrangle, Southern California	1996	U.S. Geological Survey open-file report 96-89, preliminary colour. Scale 1:24,000	
Map+Notes	Preliminary Geologic map of the Newhall 7.5' Quadrangle, Southern California	1995	U.S. Geological Survey open-file report 95-503, preliminary non colour. Scale 1:24,000	
Notes	Geologic map and Digital Database of the Apache Canyon 7.5' Quadrangle, Ventura and Kern Counties, California	2000	U.S. Geological Survey open-file report 00-359, Stratigraphy, structure and units description. NO MAP	
Notes	Preliminary Geologic map of the San Fernando 7.5' Quadrangle, Southern California: a Digital Database	1997	U.S. Geological Survey open-file report 97-163. Just a description of the adopted GIS system	
Map	Preliminary Geologic map of the Mojave Quadrangle, California	1959		scale 1:62,500
Map	Geologic map of the Lancaster Quadrangle, Los Angeles County, California	1960		scale 1:62,500
Map	State of California - Special Studies Zones. Palmdale Quadrangle	1979		scale 1:24,000 topographic map with tectonic lineaments (potentially active faults)
Map	State of California - Special Studies Zones. Ritter Ridge Quadrangle	1979		scale 1:24,000 topographic map with tectonic lineaments (potentially active faults)
Maps (13)	Topographic maps along I-5 route	-		scale 1:24,000
Maps (24)	Topographic maps along SR-14 (via Palmdale) route	-		scale 1:24,000

APPENDIX 2 GEOLOGIC SETTING

2.1 Physiography of the region

The physiography of the region is a product of the geologic history of the area. Several coastal mountain ranges underlain by severely folded, faulted, mostly metamorphosed marine and continental sediments, forming the Pacific Border and the Lower Californian Physiographic Provinces.

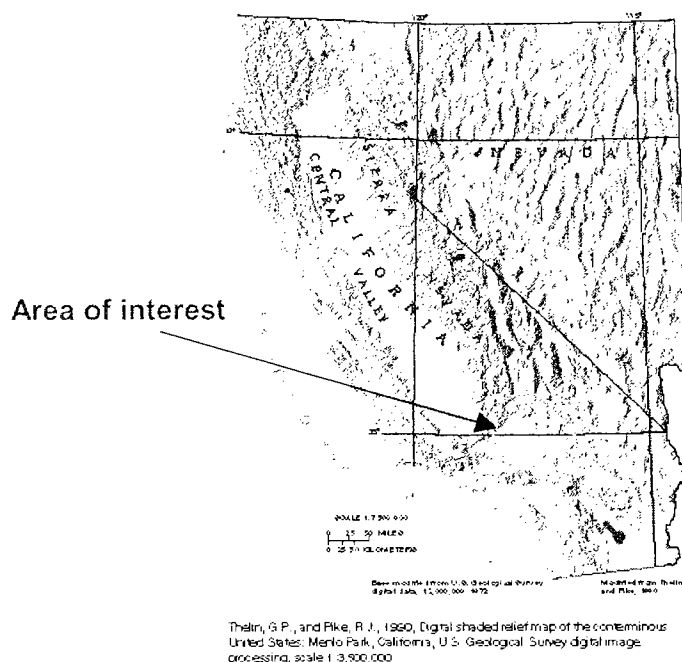


Figure A2.1 Digital, shaded relief map showing the high rugged California mountain ranges surrounding the low lying Central Valley (modified after USGS Groundwater Atlas of United States; California, Nevada)

In the interior, the granitic rocks that underlie the fault blocks of the Sierra Nevada and the volcanic rocks of the southern Cascade Mountains join to form the eastern border of the low lying California Trough, which contains the Central Valley.

East of the Sierra Nevada, the landscape is characterized by a series of low, north-south trending mountain ranges and intervening valleys; the ranges and valleys were created by faulting that resulted in the horst and graben structures which in turn formed the Basin and Range Physiographic Province.

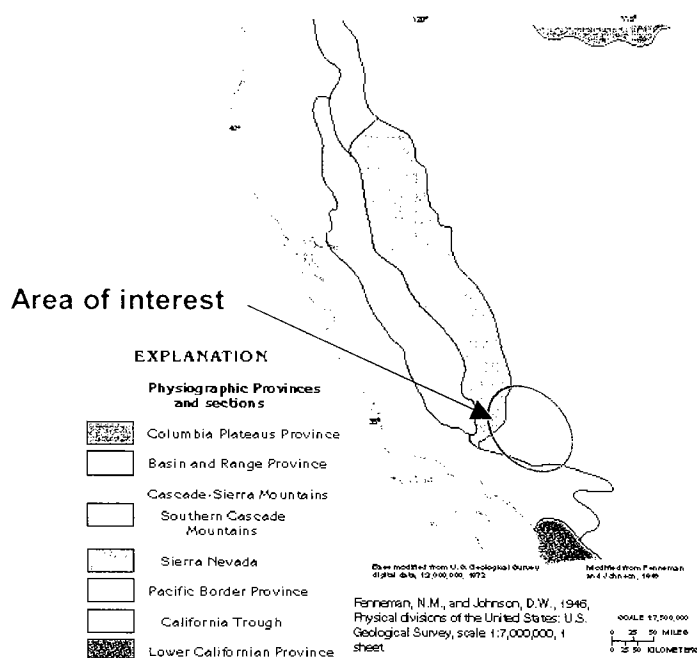


Figure A2.2 California Physiographic provinces (modified after USGS Groundwater Atlas of United States; California, Nevada).

The alternative alignment options intersect three physiographic provinces, namely: Central Valley (California Trough), Basin and Range (Mojave desert), and Pacific Border (Transverse Ranges; south of San Andreas fault alignment).

2.2 Regional structural outline

The California geographic region is situated along the active geodynamic margin between North America and North Pacific tectonic plates. The main boundary between the two plates coincides with the NNW-SSE San Andreas active fault system which separates the southern California from the rest of the north America continent.

Many other important regional active faults are present in California which determine and control the geologic development of distinct zones. The principal faults include: the NE-SW trending Garlock fault and the associated Tehachapi mountains separate the Sierra Nevada batholithic region from the Mojave desert, the complex system of San Gabriel-Santa Susana Sierra Madre faults which bound the Transverse Ranges north of Los Angeles, the San Gabriel NW-SE trending fault system which limits westward the San Gabriel mountains region, the White Wolf fault zone which intersects the southern part of the Sierra Nevada batholite.

The main faults are associated with a lateral strike slip character (San Andreas, Garlock, San Gabriel), while the minor faults are considered as compressive thrust faults (e.g., Santa Susana Sierra Madre, Pleito, and Pastoria systems) or normal type (e.g., Raymond Fault).

Practically all the above-mentioned main faults, and a significant number of minor associated faults will be crossed by the alternative alignment options. Depending on the geometric characteristics of the alignment such faults will be crossed either underground or at grade.

For the choice of the final alignment, one crucial aspect is represented by the active character of the faults. In fact, most of these faults are considered tectonically active or potentially active and seismogenetic in historic or recent (< 10,000 years B.P.) times. In this respect, California is well recognized as one of the most seismically active areas in the world. Besides, the anticipated lateral offset that could occur along major faults during earthquakes of exceptional magnitude, the design of underground structures will also have to take into consideration another important phenomenon associated with active fault zones, namely, the slow plastic slippage by which tectonic stresses are accommodated. Such movements can amount to several mm/year.

For the present study, the identification of fault zones is based on evidence from available maps (see reference documents list, Appendix 1) and on interpretation of satellite images coupled with morphologic analysis carried out on topographic maps (1:24,000 scale).

Because of their complex and long geologic history that presumably caused several lateral migrations of the principal fault plane, as well as the possible existence of multiple associated shear zones that might have been activated in different times, no attempt has been made to distinguish between the true fault planes and the associated fault affected zones, in terms of their geomechanical properties. It seems that this task might only be accomplished with the support of detailed studies and proper investigations.

Table A2.1 summarizes some characteristics of the principal faults that are considered to directly interfere with the underground sections of the studied alignments.

Table A2.1 Principal fault zones affecting the tunnels on the alternative alignments

Fault zone	Location (align., approx. chain.) (3)		Type	Attitude (dip/dip direction or strike direction)	Estimated width [m] ⁽¹⁾	Last seismic event year/magnitude] ⁽²⁾	
S. Andreas	I-5	km 78+000	S, RH	Near vertical, NW-SE	800 - 1000	1857 (south branch)	8.0
Garlock	I-5	km 70+250	S, LH	Near vertical, NE-SW	500 - 800	1992 (Mojave)	5.7
	AV	km 79+350					
S. Gabriel	AV	km 177+950 km 178+200 km 178+850	S, RH	Near vertical, NW-SE	400 - 600	Quaternary	unknown
S. Susana	I-5	? km 183+600	T	var., NW to NE	200 - 250	Late Quaternary 1971 (S. Fernando)	unknown. 6.5
	AV	km 184+200					
Pleito	I-5	km 57+700	T	var., NNW	150 - 200	345-1465 years ago	unknown
Pastoria	I-5	km 67+000	R	var., SSE	300 - 400	unknown; probably non active	
Edison	AV	km 38+600 km 40+600	N	45-75°, NNW	100 - 200	unknown; probably non active	
Legend S (strike-slip fault), T (thrust fault), N (normal fault), R (reverse fault); RH, LH (right-hand mov., left-hand mov.)							
Note (1) The figures refer to the estimated width of the fault affected zone							
(2) From SCDEC (Southern California Earthquake Data Center http://www.scdec.sccec.org/faultmap.html)							
(3) Chainage onset is assumed in Bakersfield							

2.3 Lithologic and lithostratigraphic outline

The alternative, analyzed alignments traverse a variety of geologic units which can be broadly divided in three principal groups separated by unconformities: pre-Tertiary crystalline rocks; Tertiary volcanic, volcano clastic and sedimentary rocks; Quaternary sedimentary deposits.

Pre-Tertiary crystalline rocks are composed of plutonic igneous Mesozoic rocks (ranging in composition from hornblende diorite to quartz monzonite to granite) and metamorphic Paleozoic to Precambrian rocks which generally occur as isolated bodies or as interbedded layers within plutonic rocks. The two rock groups together constitute the crystalline basement upon which all later units were deposited.

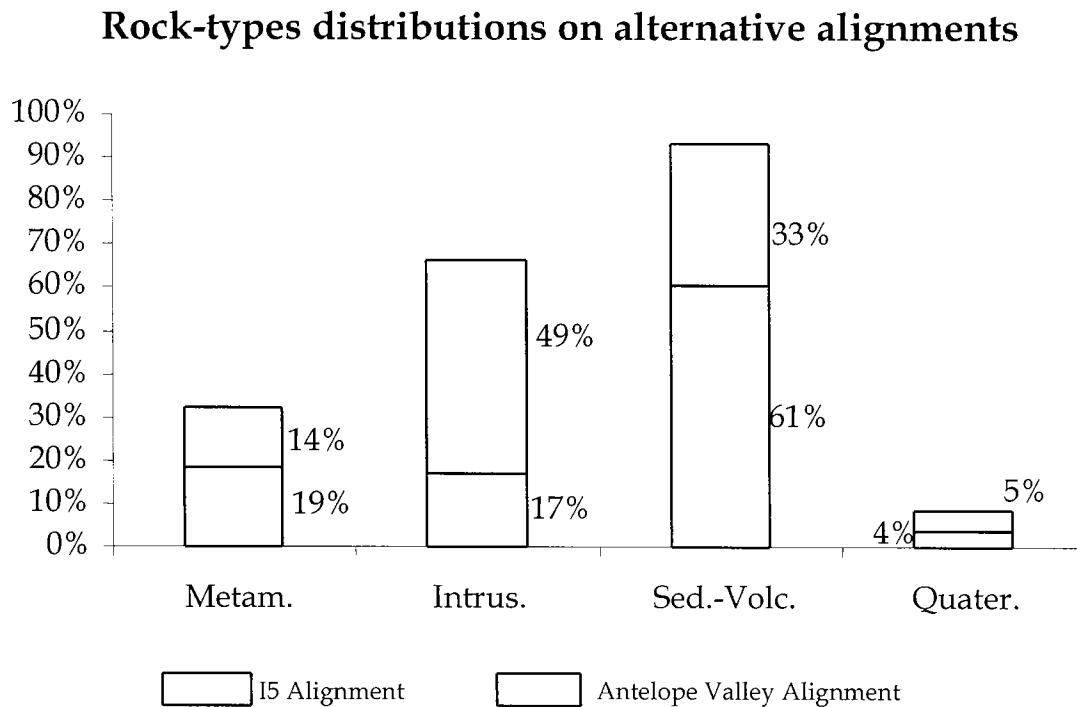
The Tertiary complex is composed of volcanic to sub-volcanic Eocene to Miocene units (rhyolite, andesite, basalt, pyroclastic rocks) and clastic flysch-like and non-marine sedimentary units (variably interbedded sandstones, siltstones, claystones and to a minor extent conglomerates).

The Quaternary deposits range from Pleistocene marine and non marine clastic deposits to fanlomeratic (i.e. sedimentary rock composed of heterogeneous unrelated materials that were originally deposited in an alluvial fan) and unlithified coarse piedmont deposits (gravel to boulder sized).

A more detailed description of the different rock-type occurrence along the alternative alignments is presented in Section 6 (Anticipated geologic conditions along alternative routes).

Figure A2.3 shows the relative distributions of different rock-types (pre-Tertiary metamorphic and intrusive rocks, Tertiary sedimentary-volcanic rocks, Quaternary deposits).

Figure A2.3 Distribution of the various rock types for the alignment options with reference to 2.5% max. grade (Metam. = metamorphic rocks, Intrus.= intrusive rocks, Sed.-Volc.= sedimentary-volcanic rocks, and Quarter.= Quaternary deposits)



Figures A2.4 gives the distribution the various rock types, in terms of both their percentage and accumulative length, on each tunnel along the I-5 alignment.

Figures A2.5 gives the distribution the various rock types, in terms of both their percentage and accumulative length, on each tunnel along the Antelope Valley alignment.

Figure A2.4 Rock type distribution in percentge and by length for each tunnel on the I-5 alternative alignment (with reference to the 2.5% max grade)

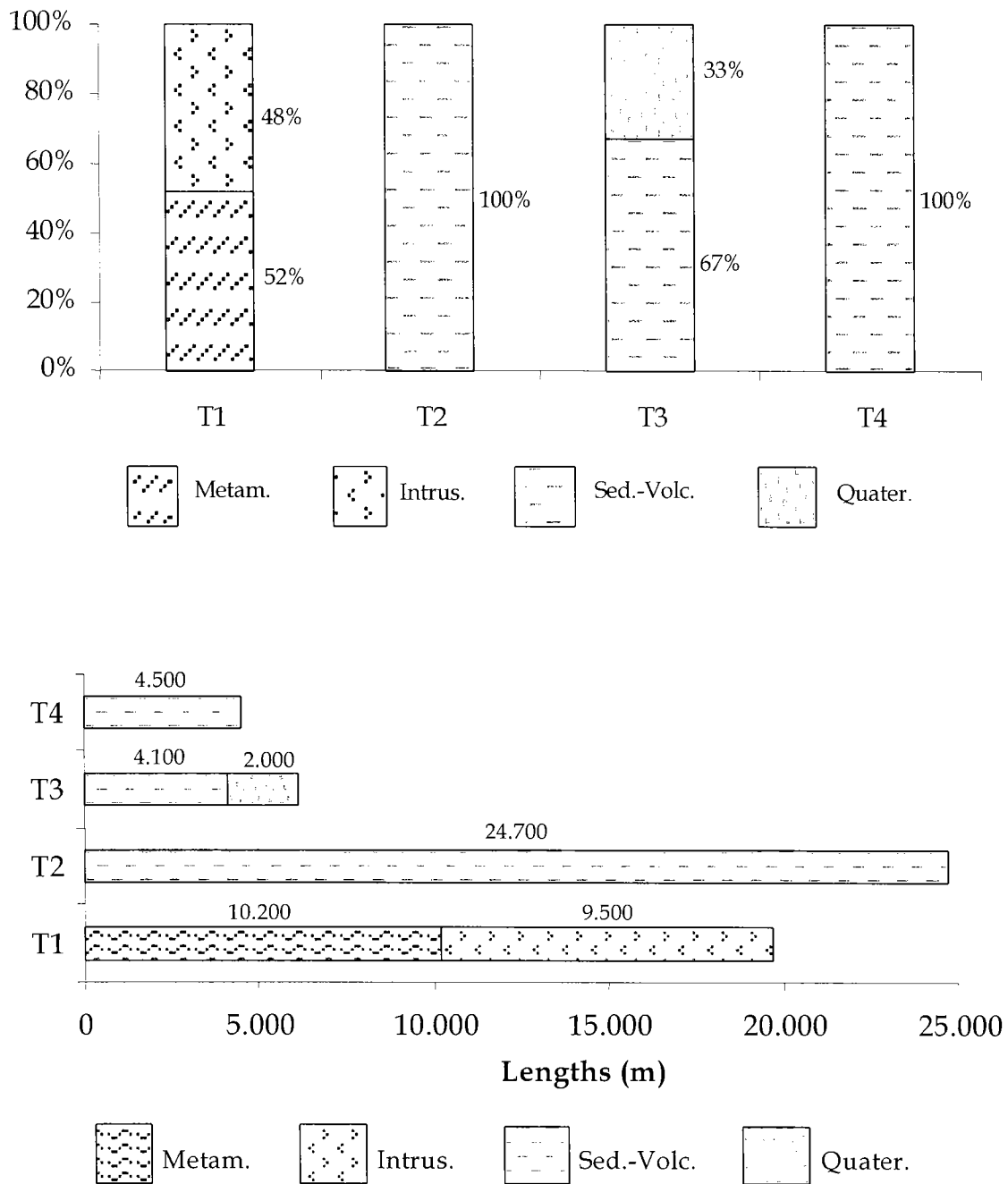
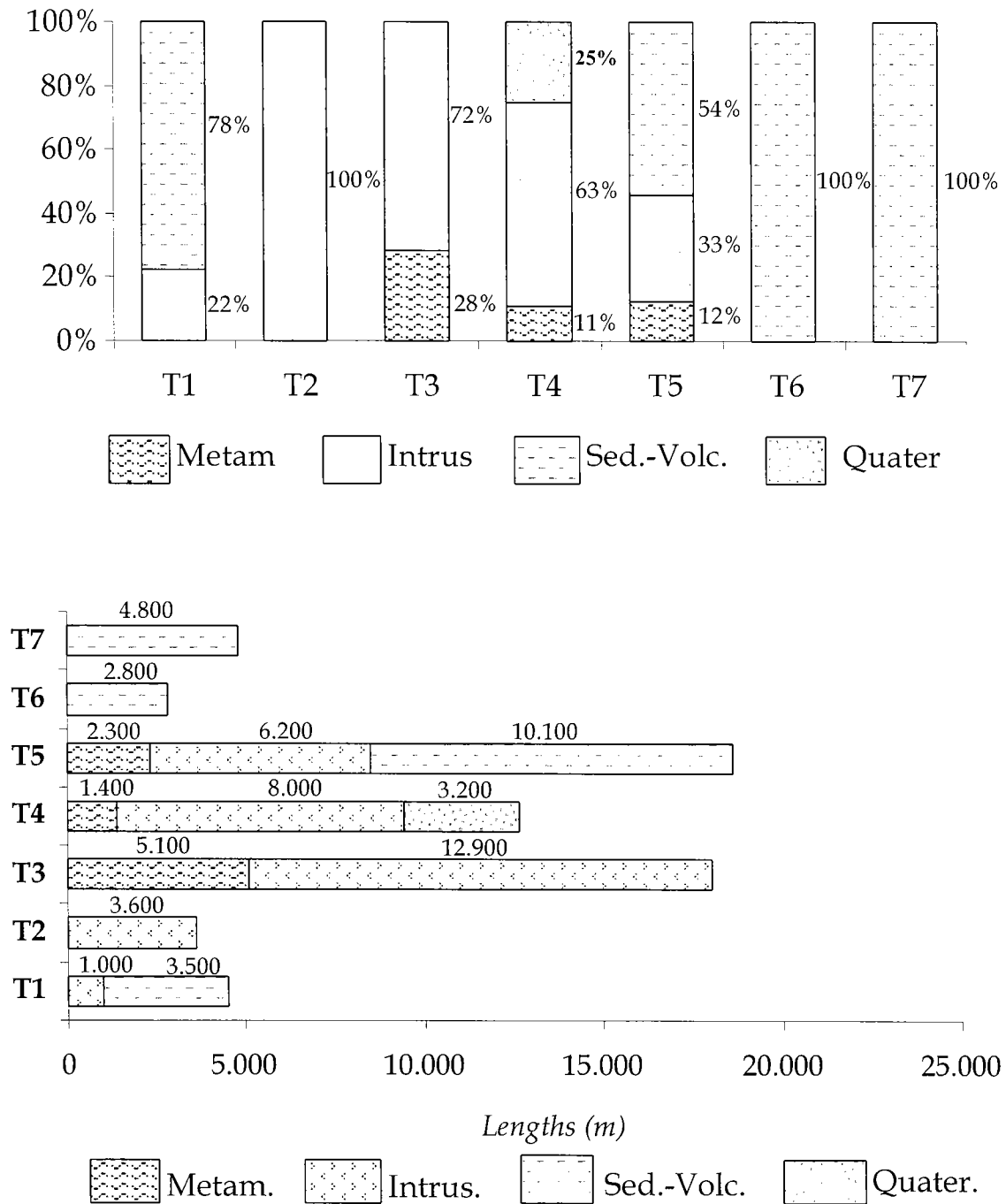


Figure A2.4 Rock type distribution in percentge and by length for each tunnel on the Antelope Valley alternative alignment (with reference to the 2.5% max grade)



The characteristics of the principal geological formations that are expected to be encountered in tunneling, for both alignment options, are described in the following sections.

Pre-Cenozoic crystalline rocks

- Precambrian anorthosites

Medium to very coarse-grained hornblende plagioclase rock; it outcrops in the San Gabriel Mountains area. It could be deeply weathered, broken and shattered with local, hard, slightly weathered to unweathered remnants. In the Soledad Canyon zone it appears to be in tectonic contact with more recent sedimentary units (Vasquez Fm).

Antelope Valley (AV) alignment (Soledad Canyon section)

- Paleozoic to Cretaceous metamorphic rocks

Moderately-foliated, fine-grained phyllites (Paleozoic) with interbedded marble and quartzite layers; this metamorphic complex is abundant towards North of Tehachapi Mountains where it is associated with younger intrusive rocks.

AV alignment

Probably of Paleozoic age highly foliated, sheared and faulted biotitic schists rich in quartz feldspar lenses are found along the Tehachapi Mountain chain where they are strictly associated with and bounded by main regional tectonic structures (Garlock fault zone).

AV alignment (Tehachapi Mountains section)

Cretaceous gneiss, amphibolite and granulite metamorphic complex is present in the northern side of the San Emigdio mountains; the complex is expected to be intensely fractured and weathered also at considerable depths. A Mesozoic to Paleozoic interlayered pile of calcareous, siliceous and pelitic rocks (Keene unit) is present along the tectonic contact between the previous metamorphic complex and the granitic rocks to the South.

I-5 alignment (Grapevine peak)

- Cretaceous intrusive rocks

In terms of relative abundance, they represent the second lithologic group as shown in Figure A2.5; they range in composition from granites, granodiorites, tonalites to quartz diorites and quartz monzonites and are known in the literature under various names. Their geomechanical properties are expected to cover the entire range (from good to very poor) of conditions in relation to specific topographic and tectonic settings.

Both I-5 and AV alignments

Tertiary sedimentary and volcanic rocks

- Vasquez Formation

It consists of coarse clastics, deposited upon volcanic rocks released as the North American tectonic plate initially collided with the Pacific Plate.

Figure A2.6 gives a typical appearance of Vasquez rock formation. The sediments at Vasquez formation were deposited above and with numerous basalt flows that constitute a major portion of the lower sequence; repeated episodes of uplift to quiescence produced several distinctive sequences called megacycles. These megacycles are characterized by coarse clastic sand and gravel deposits at the base of the sequence (as uplift became strong) with an upward fining progression (as tectonic activity slowed

down) into the siltstones and shales of a distal alluvial fan playa depositional environment.



Figure A2.6 Typical appearance of Vasquez rocks

AV alignment (Soledad Canyon section)

- Saugus Formation (Pliocene to lower Pleistocene)

Clastic sedimentary unit composed of two principal facies.

A marine Pliocene facies, composed of sandstones, mudstones, red conglomerates beds and thin limestone beds. A fluvial Pliocene Pleistocene facies, consisting of sandstones, conglomerates and siltstones, described as loosely consolidated to poorly cemented.

In the San Gabriel Mountains region, it underwent intense folding by north south directed compressional forces that were associated with the mid-Pleistocene major orogenic event of San Gabriel Mountains building.

Both *I-5* and *AV* alignments

- Ridge Basin Group (Miocene to Pliocene)

Clastic sedimentary units composed of interlayered and interfingered sandstones, siltstones and claystones; each singular lithotype can locally constitute the prevailing rock unit. The sandstone unit is highly folded, fractured and jointed in the vicinity of the major tectonic structures.

I-5 alignment

- Castaic Formation (Miocene)

Shallow marine clastic, moderately lithified unit. Prevailing facies is composed of a thin bedded claystone (crumbly where weathered) with minor, thin sandstone layers. A secondary interlayered facies is composed of fine to medium grained arkosic cohesive sandstones interbedded claystone levels.

I-5 alignment

- Towsley Formation (upper Miocene to lower Pliocene)

Fairly well indurated with lightly, well cemented interbeds of siltstones to sandstones, with local well cemented pebble conglomerate and beds of breccia. They outcrop in the Santa Susana Mountains range where they are expected to be tectonically quite disturbed. Squeezing behavior of claystone layers was reported during the 60's when the 8m-diameter Newhall tunnel was constructed.

Both I-5 and AV alignments

- Pico Formation (Pliocene to Pleistocene)

Marine siltstones, sandstones and red conglomerate beds, fairly well indurated with lightly well-cemented interbeds

I-5 alignment

Quaternary deposits

Mainly alluvial type sedimentary deposits ranging from more recent, unconsolidated, undissected valley fill (gravels to silt grained) to older slightly-consolidated deposits. The deposits can reach considerable thickness also along the piedmont areas (300 to 350 ft. exposed thickness in the Mojave zone).

Both I-5 and AV alignments

2.4 Groundwater conditions

Groundwater in the considered area is contained in three major aquifer systems which consist primarily of basin fill deposits that occupy structural depressions caused by crustal deformations. The basin-fill aquifer systems are the Basin and Range aquifers, the Central Valley aquifer system, and the Coastal Basins aquifers.

The principal water yielding units are unconsolidated, continental, clastic deposits of Tertiary age that partly fill structural basins created by faulting. Volcanic rocks, which are principally lava and pyroclastic flows of Tertiary age, are important aquifers in some sparse, non contiguous areas.

The recharge of aquifers, which occurs mainly through runoff from precipitation in the surrounding mountains, infiltrates the permeable sediments of the valley floor either at the basin margins or through streambeds.

Confined or semi-confined aquifers are also known to exist in some places, particularly where interlayering and overlapping of fine and coarse sediments do occur (e.g. in the sediment-filled tectonic depression of Antelope Valley where a deeper artesian aquifer is separated from the upper freatic aquifer through fine lacustrine clays).

For the present study no detailed hydrogeologic information was available concerning hydrogeologic regional setting in the mountainous zones: i.e., no data on the hydraulic heads, permeability distributions, flow nets, hydraulic tests. Consequently, a very qualitative hydrogeological characterization has been carried out that allowed the distinguishing of the zones in which tunneling operations could be negatively affected by

potential water inflows from the zones where hydrogeologic occurrences, if any, should not cause significant impacts.

Basement rocks (granite-like and metamorphic units) which build up the lower and lateral bound of the basin fill deposits can be normally considered as relatively impervious.

Groundwater flow through rock-like materials is basically controlled by discontinuities in rock masses; intact rocks can be considered practically impervious to water flow (due to very low primary porosity and low degree of pore interconnectivity), whereas water circulation in open fissures, joints, solution cavities is strongly facilitated.

Localized water bearing geologic structures, connected to and recharged from basin fill aquifers and from lakes and streams, are represented by areas of intense rock deformation and rupture such as folds and faults. Where the permeability of the rock material has been strongly enhanced due to tectonization, crushed basement rocks are also important water bearing features with enough effective storage and sufficient permeability to act as a local groundwater reservoir.

Anomalous hydraulic differential heads (in both vertical and horizontal directions) can develop through shear zones due to the presence of impermeable barriers made up of finegrained and weathered fault gouges. Such a condition is of particular relevance for all the numerous underground fault crossings.

2.5 Geomechanical characterization methodology

At the present stage of the study, geotechnical and geomechanical data about the geologic units that will be encountered in tunneling are not available.

In order to establish a reference geomechanical frame that permits the describing and classifying of the excavation conditions for tunneling, a simplified approach has been adopted which involves a two-step process:

- First, classify all the geologic units involved in each tunnel alignment into Geomechanical Groups according to the GSI (Geological Strength Index) system proposed by Hoek et al. (1995-2002), that is, assigning characteristic GSI-values to each unit present at the tunnel elevation and subsequently to the right Geomechanical Group;
- Then, determine the behavior class of each geologic unit according to the system proposed by Russo et al. (1998), considering not only the possible geomechanical characteristics of the unit (represented GSI) but also the corresponding in-situ stress conditions (generally, assumed to be geostatic, i.e. only proportional to the thickness of the overburden).

Practically, for Step 1 a characteristic range of GSI is attributed to each geological unit through visual comparison of its “imagined” characteristics with those shown on the special, standard charts by an experienced engineering geologist. As a result, the average, best and worst conditions are obtained. Figures A2.7 and A2.8 present two examples of such GSI charts, comparing two rock types with the standard chart (granite on Figure A2.7, and siltstones and claystones on Figure A2.8, respectively).

Figure A2.7 GSI chart for granites (after Marinos and Hoek, 2000)

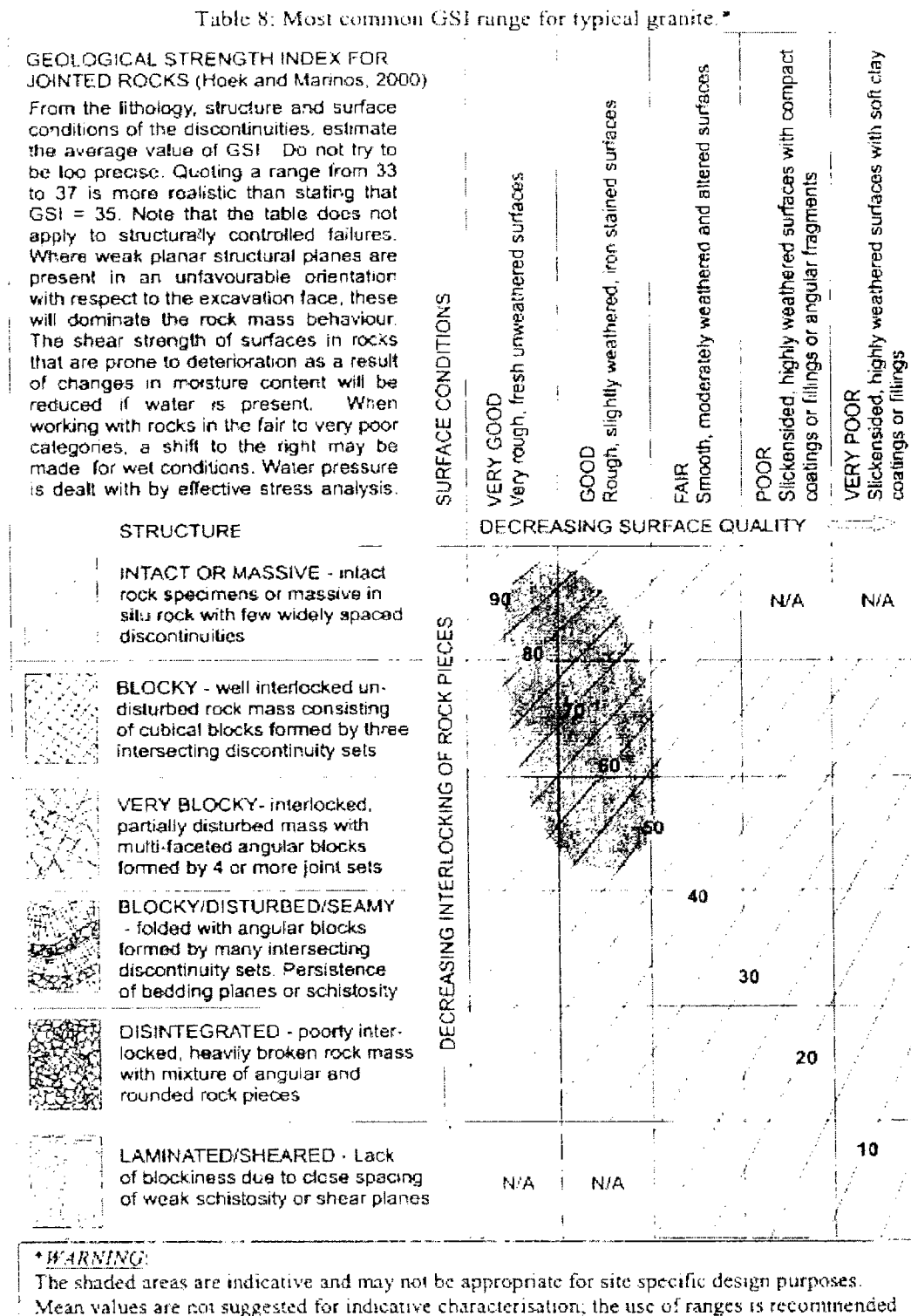
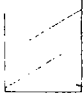
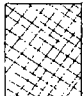



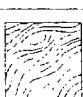


Figure A2.8 GSI chart for siltstones and claystones (after Marinos & Hoek, 2000)

Table 6: Most common GSI ranges for typical siltstones, claystones and clay shales.*

GEOLOGICAL STRENGTH INDEX FOR JOINTED ROCKS (Hoek and Marinos, 2000)		SURFACE CONDITIONS				
From the lithology, structure and surface conditions of the discontinuities, estimate the average value of GSI. Do not try to be too precise. Quoting a range from 33 to 37 is more realistic than stating that GSI = 35. Note that the table does not apply to structurally controlled failures. Where weak planar structural planes are present in an unfavourable orientation with respect to the excavation face, these will dominate the rock mass behaviour. The shear strength of surfaces in rocks that are prone to deterioration as a result of changes in moisture content will be reduced if water is present. When working with rocks in the fair to very poor categories, a shift to the right may be made for wet conditions. Water pressure is dealt with by effective stress analysis.		VERY GOOD Very rough, fresh unweathered surfaces	GOOD Rough, slightly weathered, iron stained surfaces	FAIR Smooth, moderately weathered and altered surfaces	POOR Slackensided, highly weathered surfaces with compact coatings or fillings or angular fragments	VERY POOR Slackensided, highly weathered surfaces with soft clay coatings or fillings
STRUCTURE	DECREASING SURFACE QUALITY					
	INTACT OR MASSIVE - intact rock specimens or massive in situ rock with few widely spaced discontinuities	90			N/A	N/A
	BLOCKY - well interlocked undisturbed rock mass consisting of cubical blocks formed by three intersecting discontinuity sets	80	70			
	VERY BLOCKY - interlocked, partially disturbed mass with multi-faceted angular blocks formed by 4 or more joint sets		60			
	BLOCKY/DISTURBED/SEAMY - folded with angular blocks formed by many intersecting discontinuity sets. Persistence of bedding planes or schistosity		50	40	1	
	DISINTEGRATED - poorly interlocked, heavily broken rock mass with mixture of angular and rounded rock pieces			30		
	LAMINATED/SHEARED - Lack of blockiness due to close spacing of weak schistosity or shear planes			20	2	10
		N/A	N/A			

***WARNING:**

The shaded areas are indicative and may not be appropriate for site specific design purposes. Mean values are not suggested for indicative characterisation; the use of ranges is recommended

1. Bedded, foliated, fractured
2. Sheared, brecciated

These soft rocks are classified by GSI as associated with tectonic processes. Otherwise, GSI is not recommended. The same is true for typical marls.

After the definition of geomechanical groups, the analysis of the excavation behaviour of rock masses around the excavation has been carried out, taking into account the existing stress conditions at the assumed tunnel levels.

Analysis are performed by combining the “Convergence-confinement” method (solution of Brown et al., 1983) and the probabilistic approach, through a spreadsheet model developed by Geodata (SIGRES); typical ranges for intact rock parameters, which are the necessary input to carry out such analysis (i.e., UCS, unit weight, etc.) were attributed to each rock type based on data derived from available literature. The latter is considered particularly adequate for the examined cases, in order to incorporate the actual uncertainties and the inherent variability of the geomechanical parameters.

The results of the simulations are classified on the basis of deformation indexes of the face and of the cavity (Russo et al., 1998), distinguishing six possible categories of behavior: from the best (Category “a”) to the worst condition (Category “f”). A short description of the categories follows (see also Figure A2.9).

Categories “a-b”

In the behaviour categories “a-b”, the strength of the rock mass exceeds the stress level at the face and around the cavity. The ground behaves elastically and in general deformations are of negligible magnitude. Instability phenomena are associated with wedge failure and seldom occur in category “a”, where the rock mass is considered as a continuum, but joints are relatively abundant in category “b”, where the rock mass is usually considered as discontinuous.

Category “c”

The magnitude of stress concentrations at the face approaches the strength of the rock mass (strength-to-stress ratio, S , is approximately one). The behaviour is elastic-plastic, resulting in minor instabilities. Nevertheless, the deformability gradient at the face is low, and the radial deformation (δ_o), defined as the percentage ratio of radial displacement at the face (u_o) to the equivalent cavity radius, R_o , is less than 0.5%. On the periphery of the cavity the stresses exceed the strength of the rock mass, $S < 1$, resulting in the formation of a plastic zone around the excavation, having a width less than R_o . The formation of the plastic zone results in significant convergence until a new condition of equilibrium is reached.

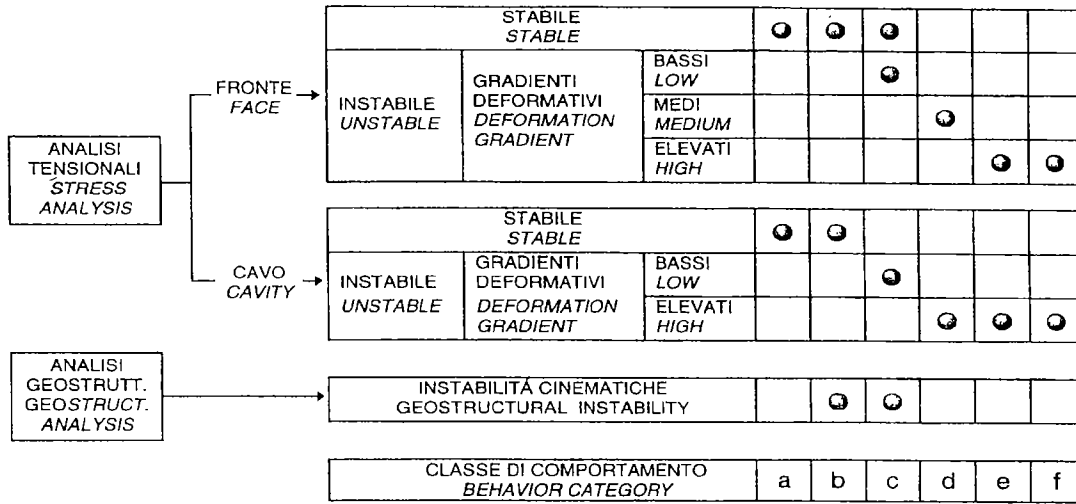
Category “d”

The magnitude of stress concentrations at the face exceeds the strength of the rock mass. The face is in a plastic state. The deformation gradient is low for typical excavation advance rates; therefore, immediate collapse of the face ($\delta_o < 1.0\%$) is prevented. The plastic state at the face in conjunction with the development of the plastic zone around the cavity results in a worse overall stability condition than that of category “c”.

Category “e”

Category “e” differs from category “d” with respect to the magnitude of deformation at the face and away from the face. At the face the stress-to-strength state results in high deformation gradient and critical conditions of face stability ($\delta_o > 1.0\%$). The width of the plastic zone is greater than R_o . Therefore, in practical terms, this category includes the highly “squeezing” condition.

Figure A2.9 Definition of the behavioural categories (after Russo et al., 1998)



Classe Category	Fronte Face	Cavo Cavity	Curve caratteristiche Characteristic curve al fronte - at the face (.....) e o distanza - at a dist. (——)	Interventi di stabilizzazione Stabilization measures	
				Funzione prev. Primary function	Tipologia Type
a	stabile stable $S > 1$ (lievi instabilità di blocchi) (limited block instability)	Stabile Stable $S > 1$ $R_p/R_o = 1$			
b	globalmente stabile globally stable $S > 1$ (cinematismi di blocchi) (wedge instability)	globalmente stabile globally stable $S > 1$ (cinematismi di blocchi) (wedge instability) $R_p/R_o = 1$		Confinamento Confinement	Radiale Radial
c	da stabile a leggermente instabile - limit condition $S \approx 1$ (bassi gradienti deformativi) (low deformation gradient) ($\delta_o \leq 0.5\%$)	instabile unstable $S < 1$ (poco spingente) (light squeezing) $R_p/R_o \approx 1-2$		>Confinamento >Confinement	Radiale Radial
d	instabile: fronte plasticizzato ma stabilità non critica not critical face instability ($S < 1$) (medi gradienti deformativi) (medium deformation gradient) ($0.5\% < \delta_o < 1.0\%$)	instabile unstable $S < 1$ (spingente) (squeezing) $R_p/R_o \approx 2-4$		Confinamento e/o miglioramento Confinement and/or improvement	Radiale ed eventualmente in avanzamento Radial and eventually in advance
e	Instabile: condizioni critiche critical instability $S < 1$ (elevati gradienti deformativi) (high deformation gradient) ($\delta_o \geq 1.0\%$)	instabile unstable $S < 1$ (spingente) (squeezing) $R_p/R_o > 4$		Miglioramento e confinamento Improvement and confinement	In avanzamento e radiale In advance and radial
f	instabile a breve termine short term stability $S < 1$ (immediate condizioni di colasso) (immediate collapse)	instabile unstable $S < 1$		Miglioramento e/o confinamento Improvement and/or confinement	In avanzamento e radiale In advance and radial

Note:

S=Rapporto di mobilitazione (resistenza/sollecitazioni)
strength-to-stress ratio

R=Resistenza mezzo nucleo - strength of half nucleus

 δ =deformazione radiale (rapporto spostamento radiale / R_o)
radial deformation defined as the percent ratio of radial displacement (u_r) to R_o δ_o =deformazione radiale scontata al fronte - radial deformation at the face R_p =Raggio plastico - plastic zone radius R_o =Raggio equivalente galleria - equivalent tunnel radius

Confinamento: Intervento teso ad evitare la decompressione della roccia e quindi il suo decadimento

Confinement: Measures to avoid relaxation and preserve the inherent rock mass strength

Miglioramento: Intervento teso a migliorare le caratteristiche geomeccaniche della roccia all'estradosso

Improvement: Measures to enhance rock mass characteristics around the cavity

Definizione delle classi di comportamento - Definition of behavior categories

(Russo et al., 1998)

Category “f”

Category “f” is characterised by immediate collapse of the face during excavation (impossible to install support). This behaviour is associated with non cohesive soils and cataclastic rock masses such as those found in fault zones, especially under conditions of high, hydrostatic pressure and/or high in-situ stresses.

With specific reference to mechanized tunneling using TBMs, as in the present case, it can be observed that “a” to “d” categories are generally not associated with significant problems for the advancement of the boring machine, while the opposite situation is related to the category “e” (highly “squeezing” condition) and category “f” (immediate collapse of the cavity).

APPENDIX 3 UNIT COSTS OF SOME EUROPEAN TUNNEL PROJECTS

The range of cost values used in the DAT analysis derives from the Consultant's experience gained from similar international projects. Table A3.1 gives a summary of the unit costs (cost per linear meter of tunnel) for different excavation methods of some European high-speed rail projects. The unit costs include the cost of excavation, temporary support and permanent support.

Specifically, the tunnels listed in the table refer to the Gotthard and Lötschberg tunnels in Switzerland, the base tunnel (also known as the Alpetunnel) of the High-Capacity Railway between Turin and Lyon, the High-Speed Railway tunnel between Bologna and Florence, the Monginevro railway tunnel at the border of Italy and France, the Somport tunnel crossing the border of France/Spain, and the Guadarrama tunnel on the High-Speed Railway in Spain.

Table A3.1 Summary of unit costs of some European tunnel projects

Tunnel (Length)	Type of Work	Excavation Method	Rock Quality	Diameter /Section	Cost (US\$/m)
Lötschberg (36km)	Railway Tunnel	TBM	Good	9.5m	7500
			Poor		19000
Gotthard (57km)	Railway Tunnel	TBM	Good	9.5m	7400
			Poor		24950
	Shaft (840m)	CONV	-	8.4m	43000
Lugano	Shaft (375m)	CONV	-	7.0m	30300
Alpetunnel (54km)	Railway Tunnel	TBM	Good	9.0m	12600
			Medium		15240
			Poor		30120
		CONV	Good	9.0m	13950
			Medium		18150
			Poor		40000
	Access Tunnel	CONV	-	70m ²	24800
Monginevro (23km)	Railway Tunnel	TBM	Good	9.0m	8000
			Medium		9850
			Poor		18100
		CONV	Good	9.0m	11200
			Medium		14000
			Poor		19800
Bologna-Firenze	Access Tunnel	CONV	-	-	14200
			-	-	-
Bologna-Firenze	Access Tunnel	CONV	Good	60m ²	8200
			Poor	90m ²	13000
Guadarrama	Railway Tunnel	TBM	Good	9.5m	10200
	Access Tunnel	CONV	Medium	75 m ²	12000
Somport	Motorway Tunnel	CONV	-	10.0m	10700

APPENDIX 4 REFERENCES

- C.A. Indermitte, H.H. Einstein. "Decision Aids for Tunnelling – SIMSUPER" User's Manual, 1998 and subsequent revisions. Department of Civil and Environmental Engineering of Massachusetts Institute of Technology.
- Clark G.B., 1987. "Principles of Rock fragmentation". Wiley & Sons, N.Y.
- G. Russo, G.S. Kalamaras, P. Grasso. "A discussion on the concepts of: geomechanical classes, behavioral categories, and technical classes for an underground project". Gallerie e grandi opere Sotterranee, March, 1998, No. 54, pp. 40-51, in both English and Italian.
- P. Marinos, E. Hoek. "GSI: A geologically friendly tool for rock mass strength estimation". GEOBEN 2000, Italy.
- E. Hoek, P.K. Kaiser, W.F. Bawden. "Support of Underground Excavations in Hard Rock". Balkema, 1995.
- E. Hoek, C. Carranza-Torres, B. Corkum. "Hoek-Brown failure criterion – 2002 edition".
- Howart K.D., 1987. "Mechanical rock excavation assessment of cuttability and boreability". Proc. RETC, New Orleans.